Journal of Electroceramics, 12, 181–186, 2004

High-ε Microwave Dielectrics in $Pb_{0.6}Ca_{0.4}Zr_{0.6+x}(Fe_{1/2}Nb_{1/2})_{0.4-x}O_3$ System

X. HU & X.M. CHEN*

Department of Materials Science & Engineering, Zhejiang University, Hangzhou 310027, China

Submitted June 11, 2003; Revised February 22, 2004; Accepted February 26, 2004

Abstract. Modification of $Pb_{0.6}Ca_{0.4}Zr_{0.6}(Fe_{1/2}Nb_{1/2})_{0.4}O_3$ dielectric ceramics was performed by Zr substitution for (Fe, Nb). The XRD patterns showed that the single phase with orthorhombic distortion unit cell was obtained in the present ceramics. The decreasing dielectric constant by Zr substitution was due to its smaller value of α/r_{ion}^3. The calculated polarizability was compared with the observed one, and the results showed a good fit, considering the polarizability of oxygen dependent on the V_{ox}. The Zr substitution on B-site reduced the temperature coefficient of dielectric constant effectively due to the reduced dielectric constant. The effects of tilting transition on the temperature coefficient of dielectric constant were also discussed. The modified microwave dielectric properties were obtained in $Pb_{0.6}Ca_{0.4}Zr_{0.6+x}(Fe_{1/2}Nb_{1/2})_{0.4-x}O_3$ for $x = 0.3$: $\varepsilon_r = 100$, $Q \times f = 3{,}300$ to $3{,}600$ GHz, $\tau_f = 6$–8 ppm/°C.

Keywords: perovskite, microwave dielectrics, polarizability

1. Introduction

With the tremendous advancement in microwave communication and microelectronic technologies, dielectric ceramics are widely used as resonators, filters, oscillators, high frequency capacitors, temperature-compensated capacitors, and so on. In such applications, high dielectric constant microwave dielectrics with near-zero temperature coefficient of resonant frequency have received intensive attention for reducing the size of microelectronic circuits [1]. Recently, The lead-based complex perovskites $Pb(B'_{1-x}B''_x)O_3$ have attracted much attention for their characteristic dielectric nature, i.e. high dielectric constant and good temperature stability around the broad diffuse phase transition [2]. Kato et al. [3] previously modified the lead-based complex perovskites by Ca^{2+} substitution for Pb^{2+} and Chen et al. [4–6] modified lead-based complex perovskites by introducing the paraelectric perovskite titanate.

In lead-based perovskites, antiferroelectrics have also received much attention for their anomalies of dielectric properties as the same as relaxors. Some research had been made on the modification of lead zirconate by adding rare-earth oxides [7]. Kato et al. [8] investigated alkaline-earth substitution for Pb in $PbZrO_3$. Chen et al. modified $PbZrO_3$ by introducing $Ca(Fe_{1/2}Nb_{1/2})O_3$ [9].

In previous work, good microwave dielectric properties were obtained in (1-x)$PbZrO_3$-$x$$Ca(Fe_{1/2}Nb_{1/2})O_3$ solid solutions for $x = 0.4$: $\varepsilon_r = 140$, $Q \times f = 1{,}776$ GHz, $\tau_f = +120$ ppm/°C [9]. In this paper, modification of 0.6$PbZrO_3$-0.4$Ca(Fe_{1/2}Nb_{1/2})O_3$ dielectric ceramics by Zr substitution for (Fe, Nb) are investigated to obtain the near-zero temperature coefficient of resonant frequency. The microstructures are characterized together with the dielectric properties.

2. Experimental

$Pb_{0.6}Ca_{0.4}Zr_{0.6+x}(Fe_{1/2}Nb_{1/2})_{0.4-x}O_3$ ($x = 0.1$, 0.2, 0.3) dielectrics were prepared by a solid-state reaction process with the columbite precursor method. $FeNbO_4$ powders were first synthesized at 1100°C in air for 3 h from Fe_2O_3 and Nb_2O_5, and then the

*To whom all correspondence should be addressed.

$Pb_{0.6}Ca_{0.4}Zr_{0.6+x}(Fe_{1/2}Nb_{1/2})_{0.4-x}O_3$ powders were synthesized by the mixtures of $FeNbO_4$, PbO, $CaCO_3$, and ZrO_2 calcined at 900°C for 3h, where the raw powders all had high purity (≥99%). The synthesized powders were batched with 4% excess PbO to account for the lead loss and then pressed into compacts of 12 mm in diameter under 98 MPa. After debinding, the samples were weighted to calculate for the PbO weight loss and then sintered at 1175° to 1325°C in air for 3 h.

Bulk density was measured by dimensional method for the sintered samples. The microstructures were characterized by X-ray diffraction (XRD) analysis using graphite diffracted beam monochromator (Rigaku D/max-3B, CuKα, $\lambda = 1.5406$ Å) and scanning electron microscopy (SEM, HITACH S-570) equipped with energy dispersive X-ray spectrometry (EDS).

Measurements of the dielectric constant and dielectric loss were conducted from 10 to 1 MHz at room temperature by an HP4284A LCR meter, and the temperature coefficient of the dielectric constant was measured at 1 MHz from room temperature to 85°C. Silver paste was used for the electrodes. The microwave dielectric properties were evaluated by the Hakki and Coleman's dielectric resonator method [10] at the frequencies of 3–4 GHz.

3. Results and Discussion

The PbO weight loss of $Pb_{0.6}Ca_{0.4}Zr_{0.6+x}(Fe_{1/2}Nb_{1/2})_{0.4-x}O_3$ ceramics with various Zr content at different sintering temperature is shown in Fig. 1. The PbO weight loss increases with increasing Zr content for the expanded unit cell and the change of chemical bond [11]. The dense ceramics with bulk density ≥95% T.D. (theoretical density) are obtained by sintering at 1175° to 1225°C due to the relatively lower PbO weight loss (Figs. 1 and 2).

In the sintered pellets, the color of sintered surface is different from that of the bulk distinctly and the sintered surface layer is observed of approximately 50 μm thick as shown in Fig. 3. Disagreeing with Saha [12], who considered the excess lead oxide would be squeezed out and got accumulated at the bottom of the sample, the EDS shows that the atomic ratio of Pb/Ca in sintered surface (0.765) is smaller than that in bulk (1.495) in $Pb_{0.6}Ca_{0.4}Zr_{0.9}(Fe_{1/2}Nb_{1/2})_{0.1}O_3$ dielectrics (Fig. 3). It indicates more severity lead volatilization

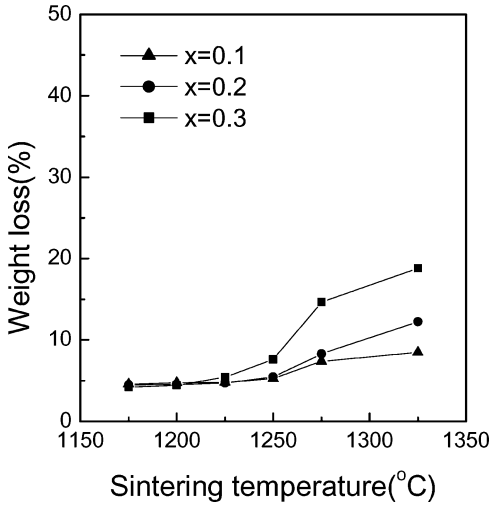

Fig. 1. The PbO weight loss of $Pb_{0.6}Ca_{0.4}Zr_{0.6+x}(Fe_{1/2}Nb_{1/2})_{0.4-x}O_3$ dielectrics with various Zr at different sintering temperature.

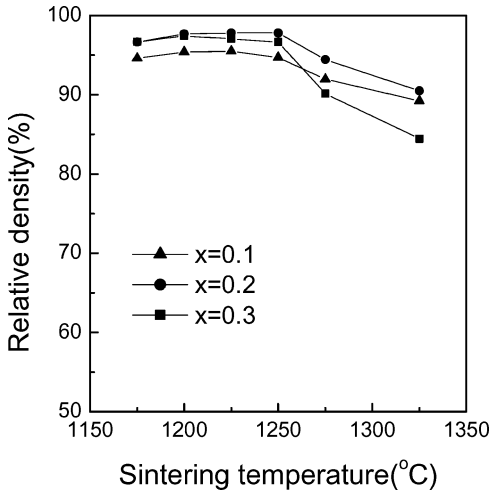

Fig. 2. The relative density of $Pb_{0.6}Ca_{0.4}Zr_{0.6+x}(Fe_{1/2}Nb_{1/2})_{0.4-x}O_3$ dielectrics with various Zr at different sintering temperature.

in the sintered surface of the samples. The excess PbO, which is expected to enter the crystal lattice, is not observed in the grain boundary by EDS analysis. So, the stoichiometric chemical composition is promised in the bulk by the excess PbO entering crystal lattice and the severity lead volatilization only existing on the surface.

X-ray diffraction patterns of the present ceramics with different composition are shown in Fig. 4. A single phase is obtained by the excess PbO

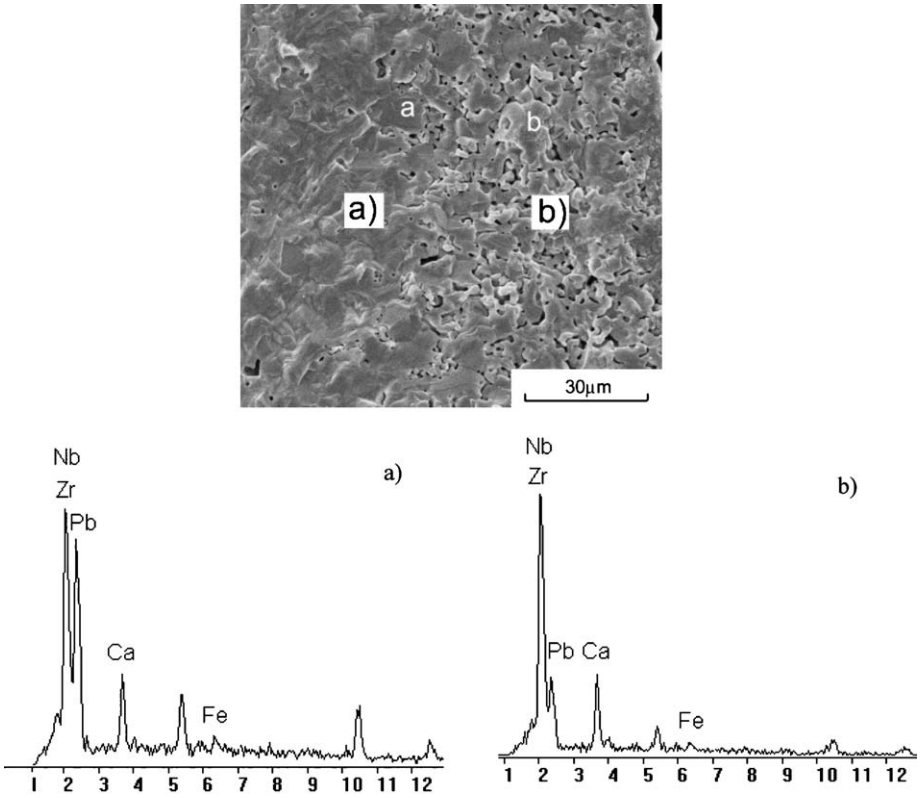

Fig. 3. SEM and EDS of fracture surface in $Pb_{0.6}Ca_{0.4}Zr_{0.6+x}(Fe_{1/2}Nb_{1/2})_{0.4-x}O_3$ dielectrics sintered at 1225°C. (a: bulk; b: sintered surface)

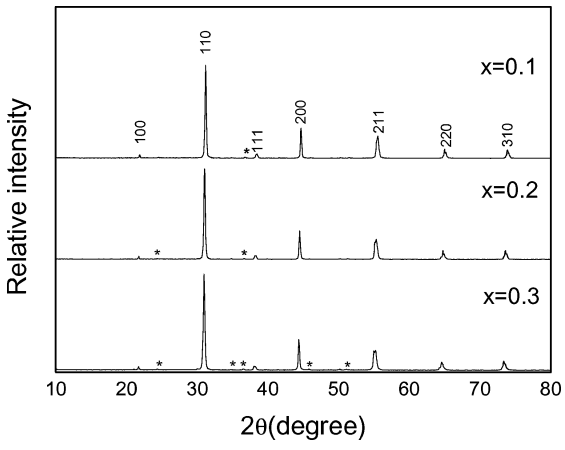

Fig. 4. XRD patterns of $Pb_{0.6}Ca_{0.4}Zr_{0.6+x}(Fe_{1/2}Nb_{1/2})_{0.4-x}O_3$ dielectrics with various compositions sintered at 1225°C.

compensation. This is different from the $PbZrO_3$-$CaZrO_3$ and $PbZrO_3$-$Ca(Fe_{1/2}Nb_{1/2})O_3$ systems where (Ca, Zr)O_2 secondary phase is found in the cause of PbO volatilization. Apart from a few extra reflections, the patterns looks very much like that from a primitive cubic structure. It is well known that antiphase tilting of the oxygen octahedra gives rise to reflections of the type odd-odd-odd, whilst inphase tilting produces odd-odd-even reflections. So, the weak $\frac{1}{2}$ (311) and $\frac{1}{2}$ (310) superlattice reflections indicate both antiphase and in-phase tilting shown in Fig. 5 and they can be indexed by tilt system $a^-a^-c^+$. The remaining superlattice reflections such as $\frac{1}{2}$ (410) and $\frac{1}{2}$ (412) reflections suggest the cation displacement in the tilting structure and the same conclusions can be obtained from the splitting (111), (211) and (220) reflections pointed by the arrows. Therefore, the phase can be assigned to the perovskite phase with orthorhombic (Pbnm) structure ($a^-a^-c^+$ tilt system) (JCPDS 82-0231).

Figure 6 shows the dielectric constant of $Pb_{0.6}Ca_{0.4}Zr_{0.6+x}(Fe_{1/2}Nb_{1/2})_{0.4-x}O_3$ with various compositions. The dielectric constant decreases with increasing Zr content. To predict the dielectric constant from the chemical composition, molecular dielectric polarizability is related to the Clausius-Mossotti

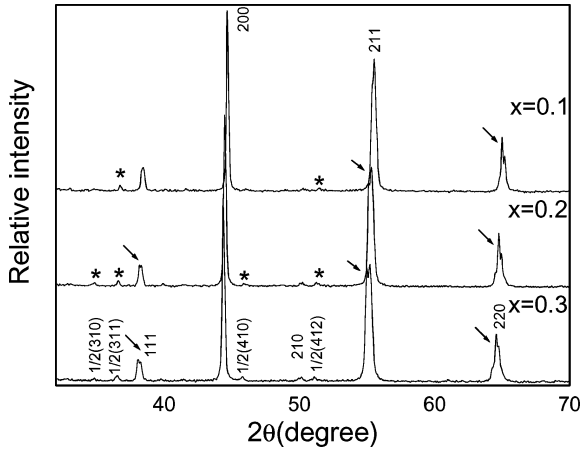

Fig. 5. XRD patterns between 32° to 70°C of $Pb_{0.6}Ca_{0.4}Zr_{0.6+x}$-$(Fe_{1/2}Nb_{1/2})_{0.4-x}O_3$ dielectrics with various compositions sintered at 1225°C.

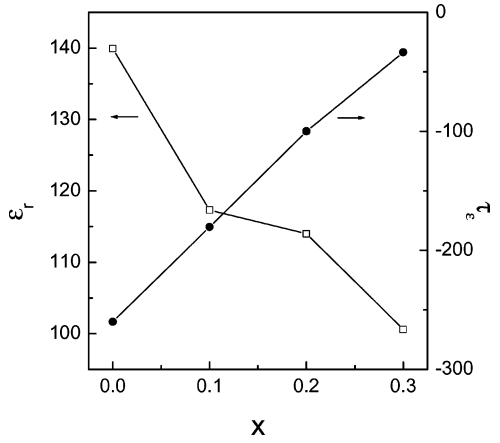

Fig. 6. Dielectric properties of $Pb_{0.6}Ca_{0.4}Zr_{0.6+x}(Fe_{1/2}Nb_{1/2})_{0.4-x}$-$O_3$ dielectrics measured at 1 MHz with various compositions sintered at 1225°C.

equation [13]:

$$\alpha_D = \frac{V_m(\varepsilon - 1)}{b(\varepsilon + 2)} \tag{1}$$

where ε is the measured dielectric constant, b is assumed to $4/3\pi$, V_m is the molar volume. Shannon et al. [13] got two series of dielectric ionic polarizabilities from the above equation considering independence or dependence of the oxygen polarizability (α_D(O)) on oxygen molar volume (V_{ox}). Shannon and Fratello et al. [13, 14] also showed that ionic polarizability correlated roughly with the cube of the ionic or crystal radius for ions of the same valence. The effective ionic radius, molecular dielectric polarizability and the ration of polarizability to the cube of the effective ionic radius are given in Table 1. The value of Zr ion for α/r_{ion}^3 is smaller than that of (Fe, Nb) and it results in the decreased dielectric constant with increasing Zr content.

Table 1. Polarizability and ionic radius for the related ions.

	r_{ion} (Å)[15]	α (Å^3)[13]	α/r_{ion}^3
Pb^{2+}	1.49 (XII)	6.58	1.99
Ca^{2+}	1.34 (XII)	3.16	1.31
Zr^{4+}	0.72 (VI)	3.25	8.70
Fe^{3+}	0.645 (VI)	2.29	8.53
Nb^{5+}	0.64 (VI)	3.97	15.14
$(Fe_{1/2}Nb_{1/2})^{4+}$	0.6425(VI)	3.13	11.80

Table 2. Observed dielectric polarizabilites, theoretical dielectric polarizabilites and their deviation $\Delta\alpha_D$ $(((\alpha_{D(mea.)} - \alpha_{D(theo.)})/\alpha_{D(mea.)}) * 100)$.

	V_{ox} (Å^3)	$\alpha_{D(mea.)}$ (Å^3)	$\alpha_{D1(theo.)}$ (Å^3)	$\Delta\alpha_{D1}$	$\alpha_{D2(theo.)}$ (Å^3)	$\Delta\alpha_{D2}$
$x = 0$	22.12	15.51	14.51	−6.44	15.66	0.99
$x = 0.1$	22.19	15.49	14.52	−6.26	15.68	1.24
$x = 0.2$	22.45	15.66	14.53	−7.22	15.73	0.41
$x = 0.3$	22.61	15.72	14.54	−7.46	15.76	0.28

$\alpha_{D1(theo.)}$ using dielectric polarizabilities considering independence of $\alpha_D(O^{2+})$on V_{ox} of the second column in Table 3 (ref. 15): $m = 0.001$, $n = 1.00$; $\alpha_{D2(theo.)}$ using dielectric polarizabilites of the first column: $m = 0.001$, $n = 2.00$; $\alpha_D(O^{2+}) = \alpha_{D0}(O^{2+}) + m(V_{ox}^N)$.

Table 2 shows the measured dielectric polarizabilites, theoretical dielectric polarizabilites and the deviation $(((\alpha_{D(mea.)} - \alpha_{D(theo.)})/\alpha_{D(mea.)}) * 100)$. The theoretical dielectric polarizabilites are calculated by the additivity rule in Eq. (2) from two series of dielectric polarizability.

$$\alpha_D(ABO_3) = \alpha_D(A) + \alpha_D(B) + 3\alpha_D(O) \tag{2}$$

The measured dielectric polarizabilites are calculated by the Clausius-Mosotti equation. The better fit on $\alpha_{D2(theo.)}$ shows that the dependence of the oxygen polarizability on oxygen molar volume must be considered to predict the dielectric polarizability in the present system, though Shannon suggested that for use with compounds having $V_{ox} > 25$ Å^3.

By differentiating the Clausius-Mosotti equation with respect to temperature, the temperature coefficient

of permittivity is obtained [16, 17]:

$$\tau_\varepsilon = \frac{1}{\varepsilon}\left(\frac{\partial \varepsilon}{\partial T}\right)_P = \frac{(\varepsilon-1)(\varepsilon+2)}{\varepsilon}(A+B+C) \quad (3)$$

where

$$A = -\frac{1}{3V}\left(\frac{\partial V}{\partial T}\right)_P, \quad B = \frac{1}{3\alpha_m}\left(\frac{\partial \alpha_m}{\partial V}\right)_T\left(\frac{\partial V}{\partial T}\right)_P,$$
$$C = \frac{1}{3\alpha_m}\left(\frac{\partial \alpha_m}{\partial T}\right)_V.$$

The term A is the linear-expansion coefficient representing the thermal expansion that results in dilution of the concentration of dipoles. The term B represents the increase in polarizability due to volume expansion attributed to an increase in rattling space and the term C represents the direct dependence of the polarizability on temperature. Cockbain et al. [16] indicates that, for the situations of dielectric constant over 10 and dielectric loss less than 0.001,

$$\tau_\varepsilon \approx \varepsilon(B+C) - \alpha\varepsilon \quad (4)$$

And it is found that τ_ε is in inverse proportion to the dielectric constant, where $\varepsilon(B+C)$ is a constant in this range. In the present system, the tendency of temperature dependence of dielectric constant versus composition is opposite to that of dielectric constant as shown in Fig. 6. The reduced temperature coefficient of dielectric constant with increasing Zr content is due to the reduced dielectric constant for the near-linear relation shown in Fig. 7. Moreover, the tilting transition also contributes to reducing the temperature coefficient of dielectric constant [18, 19]. The temperature dependence of dielectric constant for $x = 0.1$ and 0.3 is shown in Fig. 8. The deviation of straight dashed line in dielectric constant as a function of temperature arises from the octahedral tilting transition and the effect of tilting transition on $x = 0.3$ is more important than that on $x = 0.1$.

The microwave dielectric properties of the present ceramics are shown in Table 3. The improved microwave dielectric properties are obtained in the present ceramics and the $Q \times f$ value increases with increasing Zr content. According to the classical dispersion theory, microwave dielectric loss is mainly caused by Lorentz damping factor [20, 21]. With increasing Zr content, the

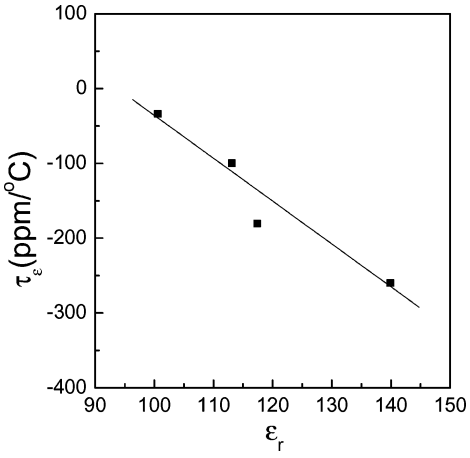

Fig. 7. Temperature coefficient of dielectric constant versus dielectric constant for $Pb_{0.6}Ca_{0.4}Zr_{0.6+x}(Fe_{1/2}Nb_{1/2})_{0.4-x}O_3$ dielectrics.

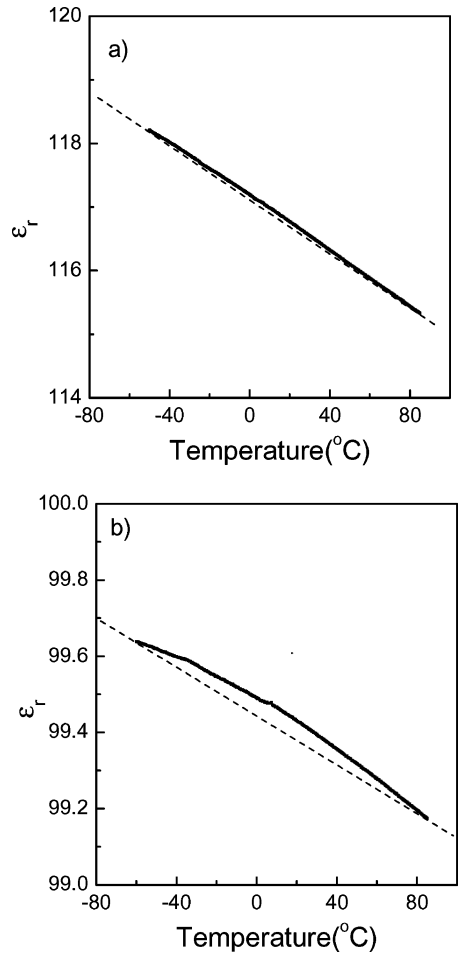

Fig. 8. Dielectric constant versus temperature of $Pb_{0.6}Ca_{0.4}Zr_{0.6+x}$-$(Fe_{1/2}Nb_{1/2})_{0.4-x}O_3$ measured at 1 MHz: (a) $x = 0.1$; (b) $x = 0.3$.

Table 3. Microwave dielectric properties of $Pb_{0.6}Ca_{0.4}Zr_{0.6+x}$-$(Fe_{1/2}Nb_{1/2})_{0.4-x}O_3$ ceramics ($\tau_f = -(\tau_\varepsilon/2) - 10$).

x	Sintering condition	f_0 (GHz)	ε_r	$Q \times f$ (GHz)	τ_f (ppm/°C)
$x = 0$	1225°C/3 h	3.02	140.7	1776	120
$x = 0.1$	1225°C/3 h	3.64	121	1916	80.1
$x = 0.2$	1225°C/3 h	3.76	113.1	2350	40
$x = 0.3$	1225°C/3 h	3.96	100.4	3300	6.8
$x = 0.3$	1200°C/3 h	3.98	100	3618	7.3

difference between positive and negative ionic radius becomes smaller, and this would decrease the Lorentz damping factor and then results in a higher $Q \times f$ value. A good combination of dielectric constant, $Q \times f$ value and τ_f is observed for $x = 0.3$ by sintering at 1200° to 1225°C: $\varepsilon_r = 100$, $Q \times f = 3,300$–$3,600$ GHz, $\tau_f = 6$–8 ppm/°C.

4. Conclusions

Modification of $0.6PbZrO_3$-$0.4Ca(Fe_{1/2}Nb_{1/2})O_3$ dielectric ceramics was performed by Zr substitution for (Fe, Nb). The $a^-a^-c^+$ tilting and cation displacement were observed according to X-ray diffraction in the present ceramics. The dielectric constant decreased with increasing Zr content, due to the smaller value of α/r_{ion}^3 in Zr ion than that in (Fe, Nb) ions. The calculated polarizability was compared with the observed polarizability, and the results concluded that the V_{ox} effect on the polarizability of oxygen must be considered. The Zr substitution for (Fe, Nb) led to the reduced temperature coefficient of dielectric constant because of the reduced dielectric constant.

By Zr substitution for (Fe, Nb), the near-zero temperature coefficient of resonant frequency was obtained in the present modified dielectrics, and the good microwave dielectric properties were obtained in $Pb_{0.6}Ca_{0.4}Zr_{0.9}(Fe_{1/2}Nb_{1/2})_{0.1}O_3$: $\varepsilon_r = 100$, $Q \times f =$ 3, 300 to 3,600 GHz, $\tau_f = 6$–8 ppm/°C.

Acknowledgment

The present work was partially supported by Chinese National Key Project for Fundamental Researches under grant No. 2002CB613302, National Science Foundation for Distinguished Young Scholars under grant No. 50025205 and Natural Science Foundation of China under grant No. 50332030.

References

1. R.C. Kell, A.C. Greenham, and G.C.E. Olds, *J. Am. Ceram. Soc.*, **56**(7), 352 (1973).
2. L.E. Cross, *Ferroelectrics*, **76**, 241 (1987).
3. J. Kato, H. Kagata, and K. Nishimoto, *Jpn. J. Appl. Phys.*, **31**, 3144 (1992).
4. X.M. Chen and X.J. Lu, *J. Appl. Phys.*, **87**, 2516 (2000).
5. X.M. Chen, X. Hu, and G.L. Hu, *Jpn. J. Appl. Phys*., **40**, 4961 (2001).
6. X. Hu, X.M. Chen, and S.Y. Wu, *J. Eur. Ceram. Soc*., **23**(11), 1919 (2003).
7. K. Tatsuki, K. Murano, T. Kawamura, H. Kato, S. Yano, and S. Nishigaki, *Proc. 6th Meet. Ferroelectric Materials & Their Application*, Kyoto 1987, *Jpn. J. Appl. Phys.*, **26** (Suppl 2) 80 (1987).
8. J. Kato, H. Kagata, and K. Nishimoto, *Jpn. J. Appl. Phys.*, **30**, 2343 (1991).
9. X. Hu and X. M. Chen, *J. Phys.: Condensed Mater*., to be submitted
10. B.W. Hakki and P.D. Coleman, *IRE Trans. Microwave Theory Tech*, MTT-8, 402 (1960).
11. T.S. Chung, H.T. Chung, and H.G. Kim, *Mater. Lett*., **27**, 111 (1996).
12. D. Saha, A. Sen, and H.S. Maiti, *J. Mater. Res.*, **11**(4), 932 (1996).
13. R.D. Shannon, *J. Appl. Phys.*, **73**, 348 (1993).
14. V.J. Fratello and C.D. Brandle, *J. Mater. Res.*, **9**, 2554 (1994).
15. R.D. Shannon, *Acta Crystallogr.*, Sect. A: Found. Crystallogr., **32**, 751 (1976).
16. A.G. Cockbain and P. J. Harrop, *Brit. J. Appl. Phys.*, **2**(1), 1109 (1968).
17. P.J. Harrop, *J. Mater. Sci.*, **4**, 370 (1969).
18. E.L. colla, I.M. Reaney, and N. Setter, *J. Appl. Phys.*, **74** (5), 3414 (1993).
19. I.M. Reaney, P. Wise, R. Ubic, J. Breeze, N.M. Alford, D. Iddles, D. Cannell, and T. Price, *Philos. Mag.*, **A 81**(2), 501 (2001).
20. G. Burns, *Solid State Physics* (IBM, Yorktown Heights, 1958, 461).
21. C.L. Huang and M.H. Weng, *Mater. Res. Bull.*, **36**, 683 (2001).